Commissioning of the 36 T Series-Connected Hybrid Magnet at the NHMFL

Mark D. Bird, *Senior Member, IEEE*, William W. Brey, Timothy A. Cross, Iain R. Dixon, *Member, IEEE*, A. Griffin, Scott T. Hannahs, John Kynoch, Ilya M. Litvak, Jefferey L. Schiano, and Jack Toth

(Invited Paper)

***Abstract*—The National High Magnetic Field Laboratory has commissioned a 36.1 T resistive/superconducting hybrid magnet with homogeneity and stability of 1 ppm over a 10 mm diameter spherical volume to be used for solid-state nuclear magnetic resonance (NMR). Most NMR magnets use single strands of superconducting wire carrying a few hundred amps and persistent joints and switches. This magnet uses a 20 kA superconducting cable in a steel conduit for the outer part of the magnet and copper-alloy sheet metal for the inner part of the magnet. While >15 hybrid magnets have been built worldwide, they typically have a field uniformity of ∼250 ppm/cm DSV and stability might be no better than 50 ppm. To attain 1 ppm uniformity, current density grading was employed in the resistive coils to cancel the z2 term. In addition, coils were shifted after the first map to reduce the z1 term. Ferroshims and resistive shims were installed in the bore to attain <1 ppm over 10 mm. The large inductance of the superconducting coil reduced the ripple sixfold compared with all-resistive magnets and essentially eliminated the 60 Hz ripple and its harmonics. An NMR lock reduced the low-frequency drift to attain ∼0.1 ppm stability.**

***Index Terms*—Electromagnets, superconducting magnets, NMR magnets, hybrid magnets.**

I. Introduction

NUCLEAR magnetic resonance (NMR) is one of the primary applications for high-field superconducting magnets. These magnets typically have more uniform and stable magnetic fields than those for other applications such as condensed matter physics as shown in Fig. 1. NMR benefits from higher magnetic fields, as the Boltzman factor at higher frequencies associated with higher fields will result in a decrease in signal averaging time in proportion to B_o^3 even for spin ½ nuclei, but the reduction in second order broadening for quadrupolar nuclei that is inversely proportional to B_o (in Hz) will result in a sensitivity enhancement that can be proportional to B_0^3 or ${B_0}^4$. Increased magnetic susceptibility will result in enhanced paramagnetic alignment of samples and even diamagnetic alignment such as the alignment of helical membrane proteins in planar lipid bilayers that is potentially enhanced with B_o^2.

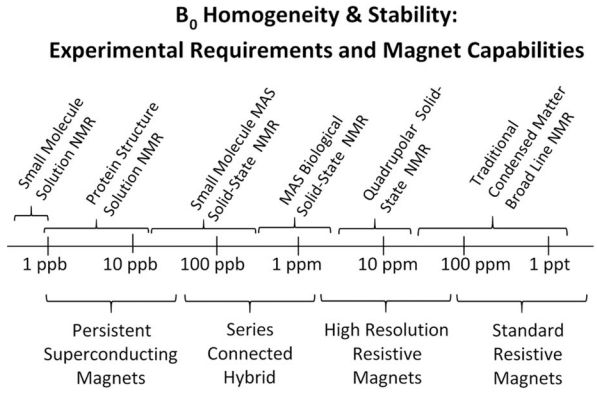

Fig. 1. The horizontal axis shows a continuous spectrum of different levels of homogeneity and stability (resolution). Above the axis are different types of physics and chemistry experiments and the resolution they require. The labels below the axis show the magnet technologies used for the highest field magnets at various levels of resolution. The SCH presently reaches better than 1 ppm which is better than has been previously attained with high resolution resistive magnets, thereby enabling a unique combination of field and resolution. We intend to continue to improve the resolution.

NMR magnets are typically superconducting with persistent joints and switches to facilitate stability as high as ∼1 ppb/hr while minimizing power consumption for experiments that frequently require tens of hours. The fields available from the magnets have increased over time as indicated in Fig. 2, reaching a plateau of 23.5 T (1 GHz H^1 resonance frequency) due to the limitations of Nb_3Sn. In the late 1990s magnet designers and NMR spectroscopists at the NHMFL proposed developing a magnet operating at 50% higher field than those previously available by using a resistive/superconducting hybrid magnet, with the resistive and superconducting coils connected electrically in series. (High temperature superconductors were not a viable option at that time.) This Series-Connected Hybrid (SCH) magnet has now been completed.

While many NMR magnets provide fields that are stable and uniform to <10 ppb, as shown in Fig. 1, there are experiments in solid state NMR and imaging of low-gamma nuclei that only require ∼1 ppm in space and time, which was chosen as the

Manuscript received August 29, 2017; accepted December 5, 2017. Date of publication December 11, 2017; date of current version January 19, 2018. This work was supported in part by the National Science Foundation under Grants DMR-0603042 and DMR-1157490, and in part by the State Florida. *(Corresponding author: Mark D. Bird.)*

M. D. Bird, W. W. Brey, T. A. Cross, I. R. Dixon, S. T. Hannahs, J. Kynoch, I. M. Litvak, and J. Toth are with the National High Magnetic Laboratory, Florida State University, Tallahassee, FL 32306 USA (e-mail: bird@magnet.fsu.edu).

A. Griffin is with the Oxford NMR, Oxfordshire, OX28 4BN, U.K. (e-mail: adrian.griffin@hotmail.co.uk).

J. L. Schiano is with the Penn State University, University Park, PA 16802 USA (e-mail: SCHIANO@engr.psu.edu).

Color versions of one or more of the figures in this paper are available online at http://ieeexplore.ieee.org.

Digital Object Identifier 10.1109/TASC.2017.2781727

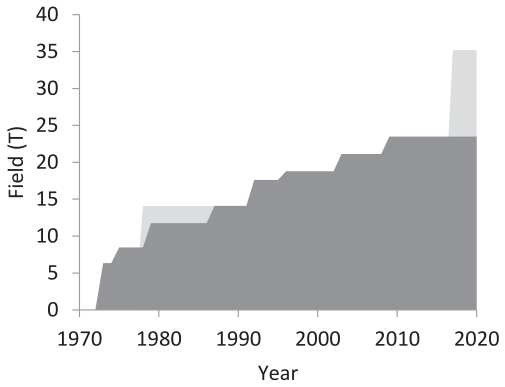

Fig. 2. NMR magnet field vs time. The dark grey represents field attained with persistent superconducting magnets. The light grey represents non-persistent magnets. The 14.1 T magnet in 1978 used Nb_3Sn tape. The 35.1 T magnet in 2017 described herein is a resistive/superconducting hybrid.

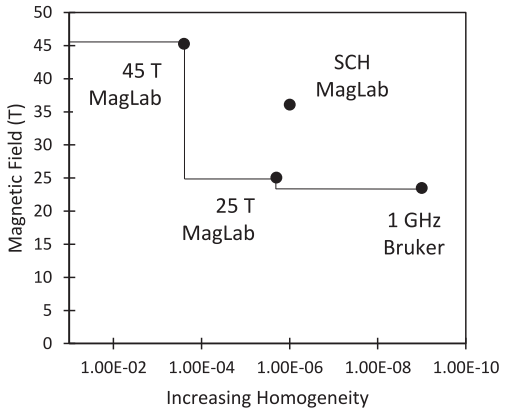

Fig. 3. Field vs homogeneity of state-of-the-art magnets. The SCH provides a combination of field and homogeneity previously unavailable worldwide.

performance requirement for this new NMR hybrid magnet. Fig. 3 presents the maximum field magnitude attained to date at various levels of precision. We see the new SCH magnet provides a unique combination of field and homogeneity worldwide.

While ∼15 hybrid magnets have been built since the earliest attempts in the mid-1970s [1], they were typically built to allow higher field within the constraints of electrical power that was available. This is one of the first times that a hybrid has been developed to enable a class of scientific experiment that was not previously routinely performed in high-field resistive magnets (another example being the magnet for neutron scattering at the Helmholtz Zentrum Berlin (HZB) [2] which was developed by the NHMFL concurrently with the SCH described herein).

II. Magnet Design

The magnet consists of four Florida-Bitter resistive coils providing 23 T while consuming 12.5 MW of dc power [3] nested in the room-temperature bore of a 13 T, 50 cm bore, 20 kA, 50 MJ, Nb_3Sn cable-in-conduit magnet [4]. A vertical cross-section is shown in Fig. 4.

While SC NMR magnets attain close to 1 ppb, this sort of uniformity is not presently attainable in a hybrid magnet for a

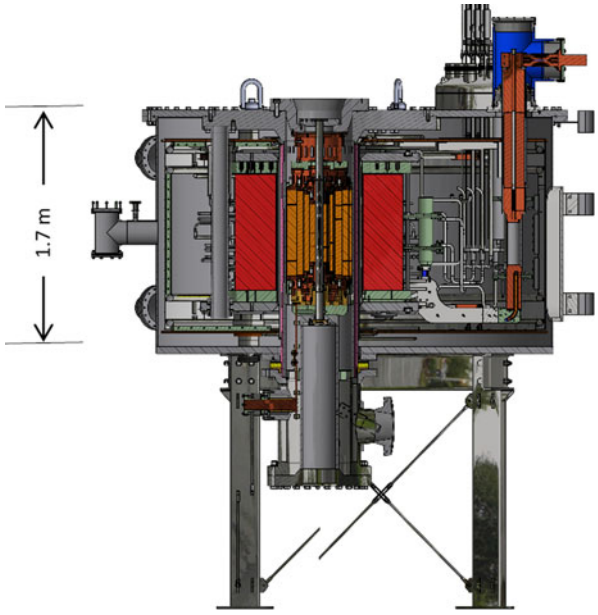

Fig. 4. SCH vertical cross-section.

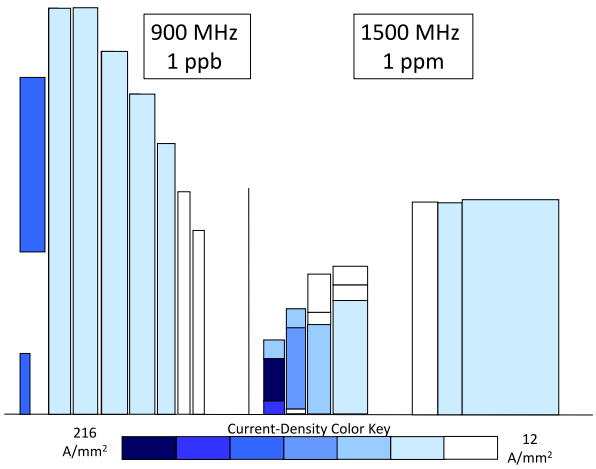

Fig. 5. Current density comparison, 21.1 T 1 ppb vs 36.1 T, 1 ppm.

few reasons. Superconductors carry less current at high fields than at low fields. Fig. 5 (left) shows the current-density distribution in the MagLab's 900 MHz (21.1 T) NMR/MRI magnet, where darker shades correspond to higher current densities. We see the current density in the outer coils is higher than in the inner ones. In contrast, Fig. 5 (right) shows the current density of the SCH magnet. Copper can carry high current density at any field. The design of the resistive magnet (inner four coils) is driven by power and stress limitations. A kiloamp of current in a small loop near the inner diameter of the coil produces higher field on the sample than the same current in a large loop near the outer diameter. However, if the current density is the same in those loops, the outer loop will dissipate more power due to its longer length. Consequently, if a resistive magnet had uniform current-density, the outer coils would make far fewer tesla/megawatt than the inner ones. By reducing the current

TABLE I
COMPARISON OF Z2 TERMS OF SCH AND SC NMR MAGNETS

SCH Coils	Z2 term (T/m^2)	900 MHz Coils	Z2 term (T/m^2)
Res A	51.9	1 (innermost)	−0.73
Res B	41.6	2	−0.80
Res C	−32.9	3	−0.93
Res D	−28.1	4	−1.14
SC	−29.7	5	−1.20
		6	−0.98
		7	−1.43
		8	−6.03
		9(outermost)	13.28
Total	2.8	Total	0.04

density of the outer coils the power is used more efficiently and maximum field/power ratios are attained [5].

With SC NMR magnets, one attains higher homogeneity via three aspects: 1) longer coils to reduce the magnitude of the field expansion terms (z2, z4, z6, etc), 2) notches and gaps to create negative field expansion terms to cancel the positive ones, 3) shimming. With resistive magnets, making longer coils is not a viable option because of the increase in power associated with it. Shorter coils, coupled with the higher current densities described above, result in the z2 terms of the various coils being larger than those typical in an SC NMR coil set as shown in Table I [5]. This means that the field uniformity is more sensitive to mis-alignment of the coils in the SCH than it is for an SC NMR magnet. In turn, this requires relying more on shimming than is standard for an SC magnet.

While ∼15 hybrid magnets have been developed previously, this is only the second to have the resistive and superconducting coils electrically in series. Fig. 6 is a schematic diagram of the 20 kA, 700 V, 50 MJ power circuit for the SCH. Like other high-current superconducting magnets built in recent years, this magnet employs binary HTS/resistive current leads using Bi2223 in a Ag/Au matrix for the HTS section.

Two unusual features of the leads are that their heat-exchangers are cooled by N_2 liquid/gas instead of GHe and that they are in the same cryostat as the main magnet (inside the iron shield) and operate in a 0.4 T fringe field. This means the HTS sections of these leads operate at higher temperature and higher field than any installed to date [6].

The final assembly of this magnet system was described previously [7].

III. SYSTEM TESTING

A. Low-Power Testing (<12 kA)

In Sept. 2016 we started energizing the magnet to modest currents. The power supply used to drive the magnet was built to operate the low-inductance (0.005 H) dc resistive magnets and its active control system was tuned for low-inductance loads. Consequently, it could not control well when the higher inductance (0.25 H) series-connected hybrid magnet was connected. A capacitor in the feedback-control system was increased 10-fold to be consistent with the new load. The system was energized repeatedly and intentionally and unintentionally dumped numerous times to test the protection hardware and software.

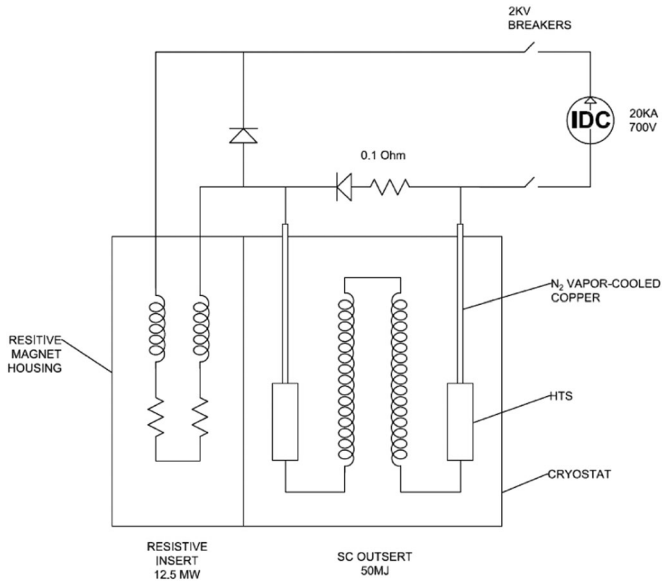

Fig. 6. 20 kA circuit for SCH. During normal operations, up to 20 kA of dc current flows from the power supply, through the resistive and superconducting coils. No current flows through the diodes. If a quench is detected, the 2 kV breakers are opened. Current then starts flowing through both diodes and the energy stored in the superconducting magnet is deposited in the 0.1 ohm resistor with a time constant of ∼2 seconds. The energy stored in the resistive magnet is discharged into its own resistance. If the resistive magnet develops a short, the protection system will measure the change in resistance and command the power supply thyristors to stop firing. A bypass diode inside the power supply will carry the current while it decays on a ∼10 second time constant.

B. High Power Testing (12–20 kA)

The breakers were intentionally opened at 18 kA to verify the system would respond as intended. We noticed that one of the commercial burst disks had buckled but did not burst. This was surprising for two reasons: the pressure was not expected to get large enough to cause a rupture and the disk should either maintain its shape or rupture. Buckling was not an expected outcome. The disk was replaced. Another burst disk was tested and found that it would not rupture at <150% of design value. The manufacturer-supplied disk mounts were faulty and we modified the design and tested one obtaining rupture at the design pressure. Modified holders were installed on the system and used while we explained the situation to the supplier and secured properly designed holders. In Berlin, rupturing of burst disks was avoided by opening the relief valves on command from the quench detection system. In Tallahassee we rely on measured pressure to open the relief valves but lowered the threshold sufficiently to prevent burst disks from rupturing. The magnet reached 36.2 T on Nov. 8, 2017 with 19.9 kA and 625 V.

C. Uniformity

To compensate the z2 and z4 terms of the magnetic field along the axis of a simple solenoid, the mid-plane of the *A* and *B* coils of the resistive insert have reduced current density (Fig. 5). There was also an extensive study of the magnitude of inhomogeneity

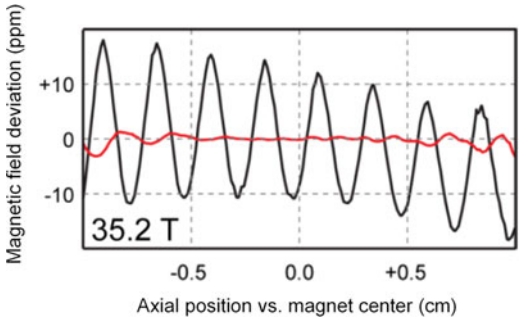

Fig. 7. SCH field map before (black) and after (red) shimming. The shimming was optimized over the middle +/−0.5 cm portion and achieved better than 1.0 ppm homogeneity over a 1 cm cylinder volume.

that can appear in the magnet due to coil mis-alignment (translation or rotation) [8]. These calculations were benchmarked by analyzing other high-homogeneity resistive magnets built in the past at the NHMFL and comparing computations with measurements prior to making predictions for the SCH. The resulting expected upper bounds on various terms were given to Oxford NMR to assess whether they believed they could build shims sufficient to provide the necessary correction.

Once the magnet was energized, the next step in pursuing 1 ppm/cm was to map the field along the axis. We saw a z1 term >100 ppm/cm, which was expected. These terms are typically present in our high-homogeneity resistive magnets due to coil mis-alignment and the gradient in the magnet temperature due to water entering at ∼10 C and leaving at ∼40 C [9]. This term was corrected by shifting the *A* & *B* resistive coils up 2.4 mm.

The next step was to perform helical maps using a differential method [5] thereby compensating for field drift during measurements. The maps showed pronounced first-order radial gradient (sinusoidal variation in map), as well as first- and second-order axial components. The combined inhomogeneity is ∼25 ppm/cm (Fig. 6). A set of ferromagnetic shims for each field of operation (23.5 = 1.0 GHz, 28.2 T = 1.2 GHz, and 35.2 T = 1.5 GHz) was developed based on the field maps. A resistive shim stack containing six first- and second-order shim terms was then inserted into the magnet bore. Fig. 7 shows that the combined ferromagnetic and resistive shims reduce the field inhomogeneity to within 1 ppm over the mapped 1 cm long, 1 cm diameter cylindrical volume [5].

D. Stability

We have previously stabilized the NHMFL's all-resistive 25 T Keck magnet to <1 ppm. As mentioned above, this SCH magnet has inductance 50 times that of an all-resistive magnet. Consequently, NMR data collected over 100 ms indicate that the field ripple is 6 times smaller in the SCH than in the Keck magnet [5].

Over longer timescales the field variation is larger. Fig. 8 shows field variation of the SCH over 200 s. The black curve is data from the magnet without active stabilization and the red trace is with active stabilization, which has reduced variation from ∼16 ppm to <0.1 ppm, much better than the 1 ppm goal [5].

Two approaches have been pursued to reach the goal of field stability of 1 ppm: 1) a modified Bruker NMR lock and 2) a combination of a pick-up coil for high frequency ripple and an NMR lock for low frequency drift [10]. The stabilized data in Fig. 8 is from the Bruker lock which has attained <1 ppm stability over periods of a few hours.

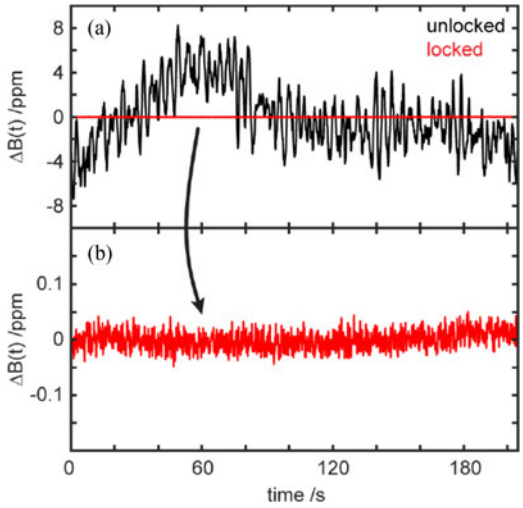

Fig. 8. Stabilization of the field of the SCH.

E. Resistive Magnet

The resistive coils have behaved quite well. The resistance vs current of the coils without the field from the SC magnet was very close to prediction [7]. When operated with the SC magnet, the resistance changed less than 1.8%, relatively low for Florida-Bitter coils in a hybrid magnet. We did however notice that the pressure drop of the cooling water for the resistive magnet decreased 1.5 bar after a few hours of water flow. This had not been noticed in previous resistive magnets at the MagLab. To date, the resistive coils have absorbed 1542, 695, 780, and 1757 MWHrs of power starting with the innermost and working outward. We believe this makes it the longest that the first set of resistive coils for a new hybrid magnet have ever lasted without repair.

F. 20 kA Joints

The joints in the CICC use a new design developed at the MagLab [11] that was previously employed in the magnet for the Helmholtz Zentrum Berlin [2] and is also being used for the 45 T for Nijmegen, The Netherlands [12]. Each of the three magnets consists of a single superconducting coil wound from five pieces of CICC. There are four internal joints (Nb_3Sn to Nb_3Sn) and two terminals (Nb_3Sn to NbTi). For the two magnets tested to date, all eight internal joints seemed initially to work well with resistances below 1 nOhm. However, one of them in the FSU magnet seems to fluctuate dramatically and sporadically. While it is typically at a normal level, its measured resistance will occasionally drift as high as 12 nOhm where it might remain for a few weeks before returning to normal. We believe this is due to an intermittent problem with one of the voltage taps. There are redundant taps that can be used if the problem persists. Of the four terminal joints, three have resistances below 0.3 nOhm while one of the FSU joints is 23 nOhm.

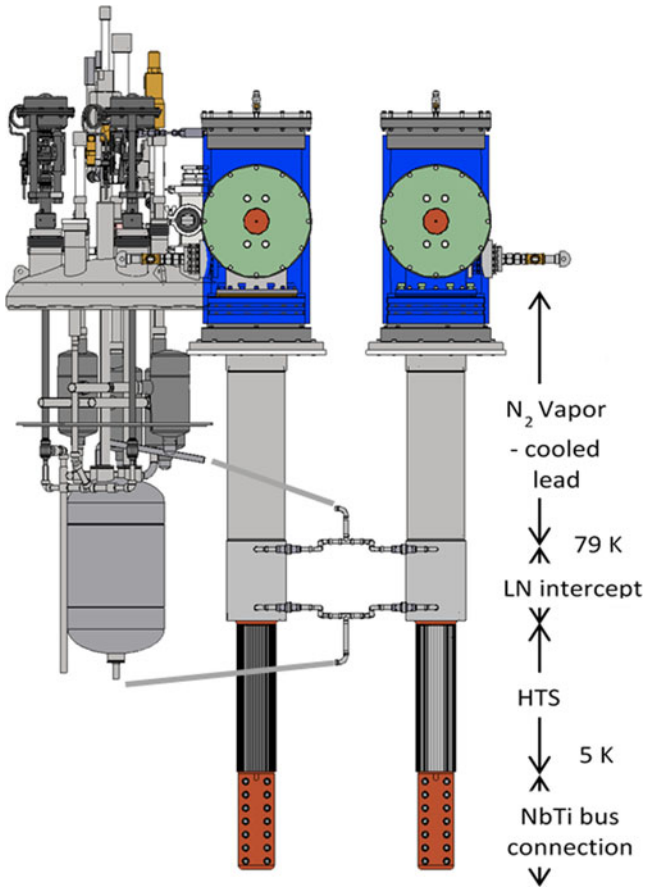

Fig. 9. 20 kA leads and N_2 cooling circuit.

G. 20 kA Binary Current Leads

The current leads are unique in operating at high temperature (N_2 cooling instead of He) and in the 0.4 T fringe field of the magnet. They are designed to operate in "self-demand" mode connected to a reservoir of 1 bar LN_2 which has active control of the liquid level and two connections to the lead intercepts, one to allow LN_2 to flow into the bottom of the intercept and another allowing gas to flow back and forth maintaining pressure and level in the two spaces. Fig. 9 shows a drawing of the reservoir and the leads.

Unfortunately, the upper of the two connections between the intercepts and the LN_2 reservoir is blocked, presumably with water-ice or LN_2. Consequently, the pressure above the liquid in the leads can be different from that above the liquid in the reservoir and the liquid levels can be different. Fortunately, the leads were designed such that it was relatively easy to install level detectors in the leads to allow monitoring of the liquid level in the leads and adjust exhaust flow rates to control it.

H. NMR Probes

To date three NMR probes have been designed and constructed for spectroscopy. Each probe has an external coil tuned for ^{7}Li. Two of the probes utilize magic angle sample (MAS) spinners to average some spin interactions to their isotropic value. One of these probes has a single broadband frequency circuit for the observe coil that is being used to detect quadrupolar resonances in both biological and material samples. The second MAS probe has a sample coil tuned for the resonance frequencies of ^{1}H, ^{13}C and ^{15}N that is being used on biological samples. The third probe is a double resonance static probe that can be used to characterize anisotropic spin interactions in powder samples or to characterize the anisotropic spin interactions in uniformly aligned samples, typically aligned membrane proteins in lipid bilayers. During the 1 year commissioning phase, since the magnet first came to field, each of these probes have produced unique data that has now been published.

TABLE II
REPEATED CHARGING RATE TEST

Up rate (A/s)	Down Rate (A/s)
9	9
9	12
12	14
14	15
16	18
18	20
20	quenched at 16 kA.

I. SHe Circuit/CICC Coil

The HZB and FSU magnets were designed to be able to ramp from 0 to 20 kA and back to 0 continuously at 30 A/s (11.1 minutes) based on calculations performed using a modified version of Gandalf software [13] and AC loss heating data collected early in the project [14]. Neither of these magnets were able to ramp at this rate without quenching. HZB found that their magnet could reach full field if charged as follows: 15 A/s from 0 to 9 kA, 2 min wait, 10 A/s from 9 kA to 18 kA, 5 min wait, 5 A/s from 18 kA to 20 kA. Discharge could use the same process in reverse without the waiting. The total time to reach field is 38.7 minutes, equivalent to ramping continuously at 8.6 A/s. After testing the HZB magnet, the Nijmegen magnet lab tested CICCs for their magnet and observed markedly higher AC losses [15], however, they were not high enough to explain the low ramp rate observed at HZB.

Testing of the FSU magnet started out using the charging schedule developed by HZB. After several months of operation we wanted to see if we have the same limitation as the HZB magnet regarding charging time. Our calculations indicated that repeated charging and discharging is more demanding than a single charge because the magnet is cold before being charged the first time while it is warmer prior to subsequent charging cycles. Hence, it may quench at the top of the second charge even if it did not in the first charge. Consequently, we decided to seek the maximum rate at which the magnet could be repeatedly charged by ramping up at one rate, coming down and back up at a higher rate, down and back up the next time at a still higher rate, etc. as seen in Table II. We were quite pleased that the magnet could be charged at 18 A/s without quenching and started normal operations the next day with 18 A/s ramp rate. The magnet quenched on the first charge cycle. The charging rate has been

successively reduced such that we are now operating at 10 A/s, faster than the original multi-speed charging routine based on HZB experience, but far slower than both what was predicted and what was demonstrated during continuous cycling.

J. Operation

The magnet is presently in a commissioning phase during which the work described above was performed as well as adjustments are being made to the N_2 and He control algorithms and power supply ramp rate, related instrumentation is being installed and tested, and procedures for training external users are being developed. A few in-house scientists are testing and debugging NMR instrumentation and collecting data using the first of the Bruker AVANCE NEO NMR spectrometers. We expect the magnet to enter normal operation for condensed matter physics experiments in 4Q2017 and for NMR users in 1Q2018.

IV. Conclusion

A unique magnet and spectrometer have been installed at the NHMFL and are being commissioned. They have met the specification of 1 ppm over 1 cm via current-density grading and a combination of ferrous and resistive shims. The combination of the large inductance of the series-connection of the resistive and superconducting coils along with an NMR lock have enabled 1 ppm stability. These systems allow solid state NMR experiments to be performed at 50% higher field than previously possible with superconducting magnets. The magnet will also serve the condensed matter physics community, particularly experiments requiring extended periods of time at high field, such as heat capacity measurements.

There are still unknown features of the magnet regarding ac losses and cooling power in the CICC that limit its ramp rate.

Acknowledgment

The magnet could not have been realized without the tireless efforts of a team of more than 40 people at the MagLab who contributed to the design, development, and fabrication of this system. In particular, the authors would like to thank J. R. Miller for developing the initial concept, T. Adkins who led the mechanical design of the CICC coil, H. Bai who led the design and construction of the cryogenic system, S. Bole who led the mechanical design of the cryostat and resistive coils, K. Cantrell who managed the system integration, P. Gorkov who was responsible for development of the NMR probes, T. Murphy who was responsible for scheduling the commissioning phase and site safety, A. Powell who developed the protection instrumentation, and H. Weijers who led the testing of the CICCs. The authors would also like to thank the various members of the CICC community who served on the external advisory committees over the years: P. Bruzzone, N. Martovetsky, J. Minervini, and A. Portone. Furthermore, the authors would like to thank a few of the >100 commercial suppliers who delivered custom materials or components for the magnet and NMR instrumentation: Bruker Biospin (field regulation), Oxford Superconductor Technology (Nb_3Sn strand), New England Electric Wire (Cabling), SMST (modified 316LN conduit), Criotec Impianti (jacketing of CICC).

References

[1] M. D. Bird, "Resistive magnet technology for hybrid inserts," *Supercond. Sci. Technol.*, vol. 17, no. 8, pp. R19–R33, 2004.

[2] P. Smeibidl *et al.*, "First hybrid magnet for neutron scattering at Helmholtz Zentrum Berlin," *IEEE Trans. Appl. Supercond.*, vol. 26, no. 4, Jun. 2016, Art. no. 4301606.

[3] J. Toth, "Resistive insert magnet designs for the series-connceted hybrid developed at the NHMFL," *IEEE Trans. Appl. Supercond.*, vol. 26, no. 4, Jun. 2016, Art. no. 4303104.

[4] Y. Zhai, I. R. Dixon, and M. D. Bird, "Mechanical analysis of the superconducting outsert for the series connected hybrid magnets," *IEEE Trans. Appl. Supercond.*, vol. 19, no. 3, pp. 1608–1611, Jun. 2009.

[5] Z. Gan *et al.*, "NMR spectroscopy at 35.2 T using a series-connected hybrid magnet," *J. Magn. Reson.*, vol. 284, pp. 125–136, 2017.

[6] W. S. Marshall *et al.*, "Fabrication and testing of the 20 kA binary current leads for the NHMFL series-connected hybrid magnet," *IEEE Trans. Appl. Supercond.*, vol. 26, no. 4, Jun. 2016, Art. no. 4801004.

[7] I. R. Dixon *et al.*, "The 36-T series-connected hybrid magnet system design and integration," *IEEE Trans. Appl. Supercond.*, vol. 27, no. 4, Jun. 2017, Art. no. 4300105.

[8] J. Toth, T. A. Painter, W. W. Brey, and K. K. Shetty, "Homogeneity study for the NHMFL series-connected hybrid magnet system," *IEEE Trans. Appl. Supercond.*, vol. 23, no. 3, Jun. 2013, Art. no. 4300104.

[9] M. D. Bird and Z. Gan, "Low resolution NMR magnets in the 23 to 35 T range at the NHMFL," *IEEE Trans. Appl. Supercond.*, vol. 12, no. 1, pp. 447–451, Mar. 2002.

[10] M. Li, J. L. Schiano, J. E. Samra, K. K. Shetty, and W. W. Brey, "Reduction of magnetic field fluctuations in powered magnets for NMR using inductive measurements and sampled-data feedback control," *J. Magn. Reson.*, vol. 212, no. 2, 2011, Art. no. 2540264.

[11] H. Bai *et al.*, "Joint design and test for the SCH," *IEEE Trans. Appl. Supercond.*, vol. 21, no. 3, pp. 2212–2215, Jun. 2011.

[12] A. de Ouden *et al.*, "Progress in the development of the HFML 45 T hybrid magnet," *IEEE Trans. Appl. Supercond.*, vol. 26, no. 4, Jun. 2016, Art. no. 4301807.

[13] L. Bottura and C. Rosso, "Finite element simulation of steady state and transient forced convection in superfluid helium," *Int. J. Numer. Methods Fluids*, vol. 30, pp. 1091–1108, 1999.

[14] R. Dixon *et al.*, "Current sharing and AC loss measurements of a cable-in-conduit conductor with Nb_3Sn strands for the high field section of the series-connected hybrid outsert coil," *IEEE Trans. Appl. Supercond.*, vol. 19, no. 3, pp. 2466–2469, Jun. 2009.

[15] A. Nijhuis and K. Yagotyntsev, "AC loss of HF Nb_3Sn CICCs for the HFML 45 T hybrid magnet," Univ. Twente, Enschede, The Netherlands, Final Rep. UT-HFML 2015-1.v2.0, Oct. 2015.